Research Article

Therapeutic Prospective of Synthesized Copper Nanoparticles using *Hemidesmus indicus* (R.Br.) on Lung Cancer cell Lines (A549) and its Antibacterial Effect against the Clinical Isolates

Deena Raj Kesari Mary, Sujatha Sukumar

Department of Biotechnology, Malankara Catholic College, Mariagiri, (Affiliated to Manonmaniam Sundaranar University, Abishekapatti, Tirunelveli), Tamil Nadu, INDIA.

Submission Date: 14-01-2024; Revision Date: 19-02-2024; Accepted Date: 23-04-2024.

ABSTRACT

Background: Research into natural chemicals and nanotechnology has attracted considerable interest in the pursuit of novel treatment methods for infectious diseases and cancer. **Aim:** The current study intended to synthesize and analyse the potential of Copper Nanoparticles (CuNPs) with the aqueous extract derived from the Indian sarsaparilla leaf, *Hemidesmus indicus* (R. Br.). **Materials and Methods:** Apart from the current research was focused on characterizing the synthesized copper nanoparticles, utilized multiple analytical techniques, including UV, FTIR, SEM, SEM-EDAX and TEM. The synthesized nanoparticles that possessed the potential antimicrobial activity were performed against the nine organisms and compared with the crude plant extract. It was found that the nanoparticles exhibited a significant zone of inhibition than the crude plant extract. Moreover, examined the potential ability of the synthesized CuNPs using *H. indicus* (R.Br.) on MTT analysis performed in lung cancer cell lines (A549). Apart from the anticancer study further revealed that apoptotic induction of synthesized nanoparticles treated in vitro cell-based apoptosis progressed to its late stage, Cells emitted orange fluorescence, signifying condensation of chromatin or fragmentation, leading to uniform red/orange-stained nuclei of cells. **Results:** The significant nuclear changes seen in *H. indicus* CuNP-treated cells, such as condensation of chromatin and nuclear disintegration, further confirmed the trigger of cell death through apoptosis. Furthermore, to elucidate the molecular level alterations of significant candidate anti-apoptotic targets-AKT and mTOR, the gene expression analysis was performed using RT-PCR. Notably, the current research results proved the efficacy of the synthesized copper-based nanoparticles from *H. indicus* in lung cancer A549 cells by initiating the apoptotic progression compared to the crude plant extract. It was well proven by apoptotic staining assays and molecular level analysis. **Conclusion:** The present findings highlighted the promising visions and therapeutic potential of the combination of nanoparticles of copper coupled with the aqueous extract, hence *H. indicus*-based nanoparticles possessed empirically antimicrobial effect and anti-cancer properties.

Keywords: *H. indicus,* Copper nanoparticle, Lung cancer, Crude extract, Gene expression

Correspondence:

Mrs. Deena Raj Kesari Mary
Department of Biotechnology, Malankara Catholic College, Mariagiri, (Affiliated to Manonmaniam Sundaranar University, Abishekapatti, Tirunelveli-627012), Tamil Nadu, INDIA.

Email: deenaanto333@gmail.com

SCAN QR CODE TO VIEW ONLINE

www.ajbls.com

DOI: 10.5530/ajbls.2024.13.16

INTRODUCTION

Natural chemical and nanotechnology research has garnered significant attention in the search for innovative treatment techniques against infectious illnesses and cancer. One specific plant that has piqued interest in traditional medicine is *H. indicus*, referred to as Indian Sarsaparilla, due to its wide array of pharmacological qualities. Traditional Ayurvedic

medicine has long recognized the numerous benefits of H. indicus, attributing its powerful anti-inflammatory, hypoglycemic, antipyretic and hypolipidemic properties.[1,2] *Hemidesmus indicus* roots, with their woody structure, offer a cooling effect and exude a pleasant phenolic flavour and fragrance.[1] This experimental plant species is extensively distributed throughout India and boasts many essential oils and phytosterols in its composition. A noteworthy chemical compound found in the roots of this plant is 2-Hydroxy-4-Methoxybenzoic acid (HMBA), which has been isolated and proven to have strong anti-diabetic, antibacterial and antioxidant activities. The high phytochemical content and documented potent activities of the *H. indicus* plant suggest its potential use as a reducing agent in the metal nanoparticles manufacturing process. Notably, silver and zinc metals have been successfully synthesized into nanoparticles using *H. indicus* as a green plant source, particularly using its leaves, stems and roots.[3]

Concurrently, CuNPs have appeared as promising candidates for numerous biological applications. Kumar *et al*., 2016; Shankar *et al*., 2019 previously described the antibacterial and anticancer characteristics of synthesized CuNPs with *H. indicus* extract, with a particular focus on their potential impact in lung cancer cells, while also exploring the associated alterations in gene expression of anti-apoptotic genes. *H. indicus*, a perennial herb, only because of the plethora of bioactive phytoconstituents such as alkaloids, flavonoids and triterpenes, which contribute to its proven antibacterial efficacy against a range of microbial infections. Previously, Iadav *et al*., 2001 described the inherent properties of *H. indicus*, including its anti-inflammatory and immunomodulatory characteristics, which position it as a potential agent for combating infectious disorders. While extensive research has also been done by several researchers about crude extract applications, investigations into the manufacturing process of nanoparticles with different metals and their antitumour potential, specifically its effectiveness against lung cancer, remain relatively scarce in scientific literature.[4-6] Given that lung cancer poses a significant global health concern with the low efficacy of current advanced therapies, researchers are aiming towards alternative approaches. Understanding the impact of *Hemidesmus indicus* on gene expression within lung cancer cells is vital for elucidating the molecular mechanisms underlying its therapeutic actions.[7]

The integration of CuNPs with natural substances opens the potential for a synergistic medicinal strategy. However, the precise synergistic effects of these entities in the context of lung cancer therapy and their impact on gene expression remain largely unknown, necessitating further investigation. Studying the gene expression changes resulting from the synthesized CuNPs using *H. indicus* (L.) R.Br. extracts of lung cancer cells will provide a crucial understanding of the molecular mechanisms governing their anticancer activities. This insight can lead to the invention of more effective and specific lung cancer treatment regimens, benefiting patients all over the world.

MATERIALS AND METHODS

Plant collection

H. indicus plant root samples were obtained from Kaliakkavilai. The root sample was powdered and stored in an aseptic condition.

Preparation of plant extract

Preparation of plant extract and Synthesis of CuNPs

250 mL of distilled water was combined with 25 g of plant powder and boiled for 1 hr at 60ºC. After cooling to room temperature, the extract was filtered using Whatman filter paper no.1 and refrigerated. Copper sulphate and plant extract were employed as precursors in the manufacturing process of Cu nanoparticles. The production process for CuNPs was prepared through magnetic stirring with optimum heating for the reaction. A copper sulphate solution (50 mL) was added with 150 mL of plant extract and shaken well until the colour changed to dark green and brown precipitation at the end. Synthesized nanoparticles were collected and rinsed utilising distilled water to eliminate impurities and then dried out at room temperature to achieve the powdered state of CuNPs.[8]

Characterization of synthesized CuNPs

To comprehend the morphological features of the manufactured CuNPs, certain analytical-based methods were carried out.[9] Characterization methods include Bio spec Nano (Shimadzu), which measures the surface plasmon resonance of nanoparticles. ATR-FTIR spectrometer was utilised to regulate the functional group of extracts accountable for decreasing the silver nitrate and consequently for forming the nanoparticles (Shimadzu IR affinity). These particles have been enclosed in an ATR (ZnSe) substrate. The crystalline nature of nanoparticles has also been studied by the X-ray diffractometer (XPERT-PRO). The scanning electron microscope (FESEM, TESCAN) and transmission electron microscope (JEOL Ltd., Japan) were employed to figure out the surface characteristics of the nanoparticles. The particle size and zeta potential in liquid suspension were both assessed using the Zetasizer Nano ZS (Malvern Instruments).

Anti-microbial activity

The primary resolution of the research was to evaluate the effectiveness of synthesized CuNPs using *H. indicus* extract in combating a broad spectrum of bacterial pathogens, which included both gram-negative and gram-positive strains, as well as fungi. To ensure a sterile environment, the autoclaving on the medium, reagents and glassware at a temperature of 121ºC for 20 min was performed. The bacterial pathogens and fungi were obtained from Clinbiocare Technology, Research Centre, Tenkasi and sub-cultured for 24-42 hr at 37ºC in a selected medium broth. To conduct the antimicrobial experiment, a fresh overnight broth culture was utilized on a Muller Hinton Agar Medium (MHA) in a petri dish. The surface of the medium was evenly covered with a sterile autoclaved cotton swab and the plates containing the bacterial strains were left to dry for a short period. Using a sterilized cork boring tool with a diameter of approximately 8mm, wells were created on the MHA medium. To conduct the antibacterial experiment, multiple test solutions were employed, including green-generated CuNPs with plant extract, crude plant extract in predetermined quantities and Ampicillin (25 mcb disc) as a positive control. Subsequently, the Petri dishes were placed in a chamber set at 37ºC for about 24 hr and the clear zone of inhibition (ZOI), which represents the area surrounding the antimicrobial agent where bacterial growth was inhibited, was measured in millimetres. The nanoparticles that exhibited antibacterial properties effectively dispersed into the MHA agar medium, thereby inhibiting the growth of the test strains. To measure the ZOI, a ruler was utilized and the measurement was taken from the bottom of the Petri plate without opening it, adhering to strict experimental procedures.[10]

Cytotoxicity study on A549 cancer cell line

Cell culture

The A549 cell lines were bought from the National Centre for Cell Sciences (NCCS) in Pune, India. Dulbecco's Modified Eagle Media has been supplemented with 10% foetal bovine serum to maintain cell viability. Antibiotics, including penicillin (100 U/mL) as well as streptomycin (100 µg/mL), were employed alongside the medium. These cell lines were maintained in humid conditions containing 5% CO_2 at 37ºC.

Cell viability assay

To examine the effects of a plant extract and nanoparticles on A549 lung cancer cell lines, a series of experiments were conducted using various concentrations of both crude plant extract and synthesized CuNPs using H. indicus (L) R. Br. extract (100, 150, 200, 400 and 600 µg/mL) for 24 hr. The experiments were carried out repeatedly thrice to ensure the accuracy and reliability of the results. Following the 24 hr incubation period, the cell viability was assessed using the MTT assay. This analysis involved the addition of MTT to each well of the microplate. By utilizing this assay, the viability of the cells will be determined and any potential changes induced by the crude plant extract and synthesized nanoparticles. This comprehensive approach sheds light on the impact of these substances on A549 lung cancer cells and allows for a more thorough analysis of their effects. The cytotoxicity of the chosen nanoparticles on A549 cells was carried out following Riss *et al* 2004. Further values for IC50 were determined using the MTT assay.

AO/EB staining

A549 cells were placed at 5x104 cells for each well in a plate of six wells as well as maintained for 24 hr. After 24 hr of being treated with HI-CuNPs (10 and 15 µg), cells were separated, rinsed using PBS, and stained by a combination of a 1:1 ratio of AO (100µg mL-1) and EB (100µg mL-1) at room temperature for 5 min. A fluorescent microscope was used to study the stained cells at a magnification of 20x. Dual AO/EB fluorescent staining is a widely employed technique that enables the identification and examination of crucial morphological alterations occurring in apoptotic cells. By utilizing this method, we can distinguish between early apoptotic cells, late apoptotic cells, necrotic cells, and normal cells therefore providing a comprehensive understanding of various stages of cellular death. Consequently, AO/EB staining has emerged as a dependable and versatile approach for accurately detecting apoptosis in cellular or tissue samples. Furthermore, its reliability lies in its ability to not only identify the presence of apoptotic cells but also to provide valuable insights into the extent and distribution of apoptotic cells within a given sample.

DNA fragmentation assay

The DNA from the control and treated A549 lung cancer cell lines (Control and 311 µg-plant extract/32 µg-synthesized copper nanoparticle) were taken for analysis as per the manufacturer's protocol (Apoptotic DNA Ladder kit, Roche, Basel). The A549 cell lines were first implanted into the six welled microplates, after which 15 µg/mL of crude plant extract and CuNP were added. Following the 24 hr incubation period, the culture medium is then taken, and the cells are retrieved by scraping around 1 mL of Phosphate-buffered solutions. Further, the steps were carried out using the kit protocol as suggested by the instructions

of the manufacturer. The final eluted DNA was run in a 1% agarose gel electrophoresis to visualize the banding pattern in the treated cells.

Quantitative real-time PCR

RNA was obtained from untreated and treated (Control and 311µg-plant extract/ 32µg-synthesized copper nanoparticle) A549 cell lines by using an RNeasy kit (Qiagen, USA) as per the guidelines by the manufacturer. Quantitative Real-Time PCR (qPCR) analysis was performed by using Quantitect Reverse Transcription and SYBR-Green mix (Qiagen, USA) on Rotor-Gene Q 5plex HRM Platform (Qiagen, USA) for measuring the expression of mRNA of two genes (PI3K and mTOR) and the primers utilised for qPCR analysis are mentioned in Table 1. Universal thermal cycling conditions were followed as described earlier.[11]

Table 1: RT Primer Sequences for selected targets

Sl. No.	Primer Name	Primer Sequence
1	ACT F	GATGATGATATCGCCGCGCT
	ACT R	CCTCGTCGCCCACATAGGAA
2	pI3K F	GTATCCCGAGAAGCAGGATTTAG
	pI3K R	CAGAGAGAGGATCTCGTGTAGAA
3	mTOR F	GTGGAAACAGGACCCATGAA
	mTOR R	CCATTCCAGCCAGTCATCTT

RESULTS

Researchers are fascinated by nanoscale materials due to their unique optical features. Nanoparticles take on a variety of hues throughout their production. Plant extracts include a variety of phytochemicals that produce copper nanoparticles by a reaction with copper sulphate. The key indicator of CuNP generation is a shift in colour from blue to brown within an hour of the reaction. After 24 hr, the colour change ceases and the nanoparticles precipitate, showing that the synthesis process is completed. Examining the produced CuNPs, UV-Vis absorption spectra were collected at various wavelengths spanning from 200 to 600 nm. These nanoparticles were created using copper sulphate and *H. indicus* leaf extract as reduction agents. It is worth mentioning that the *H. indicus* leaf extract contains physiologically active phytochemicals that play a significant role in the green manufacture of CuNPs. The absorption peak resulting from the synthesis process was observed at 443 and 586 nm, as clearly shown in Figure 1 which provides a visual representation of this phenomenon.

In addition to studying the UV-Vis absorption spectra, the FT-IR spectrum was also utilized in this research to determine the functional categories of the active components by considering its peak value of the infrared region. The findings regarding the FT-IR peak values and corresponding functional groups are accurately displayed in the comprehensive Figure 1, enabling a detailed examination of these important results. The information derived from the FTIR spectra is particularly valuable as it demonstrates that the *H. indicus* aqueous leaf extract possesses specific functional groups, including hydroxyl, carboxyl, or amine groups, which are known to contribute to the synthesis of CuNPs. These groups within the leaf extract can serve as reducing agents, facilitating the transformation of copper sulphate into CuNPs. The presence of such active phytochemicals in the *H. indicus* leaf extract further supports its potential significance for the eco-friendly manufacturing of CuNPs.

Overall, the combination of UV-Vis absorption spectra and FT-IR analysis has provided compelling evidence to suggest that the *H. indicus* leaf extract contains key comp *H. indicus* CuNP (in cm) onents essential for the successful manufacturing of CuNPs

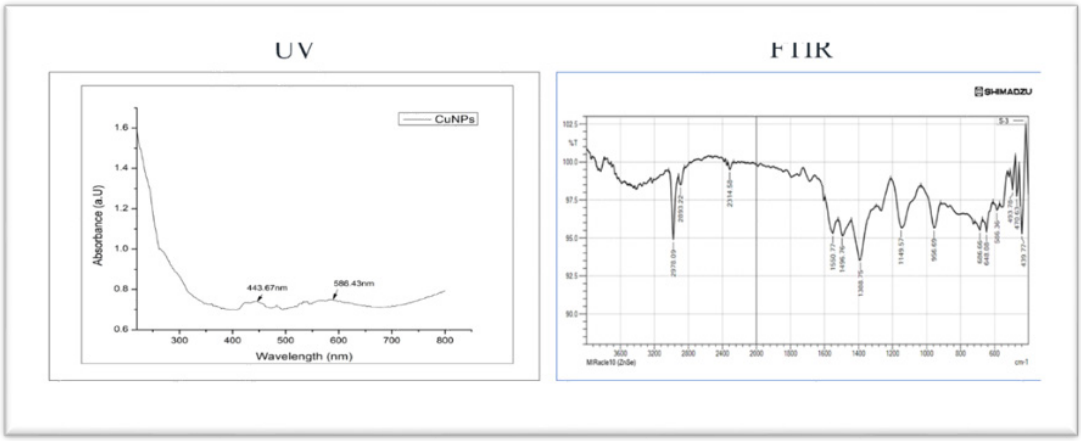

Figure 1: UV-visible spectra and FTIR spectrum of green synthesised CuNPs with *H. indicus*

These findings give a broader comprehension of green manufacturing processes and the utilization of natural resources in nanoscience and technology. In Figure 1, the FTIR spectra of CuNPs produced by *H. indicus* are presented. The spectra were recorded between 601 cm^{-1} to 555.50 cm^{-1}, revealing various interesting features. Notably, the NP peak of Plant extract is visible at 601 cm^{-1} and 555.50 cm^{-1}, providing evidence of C-I stretching. Furthermore, the existence of a peak at 1643.35 cm^{-1} suggests the involvement of C = C stretching and unsaturated ketones, indicating the presence of certain chemical compounds in the nanoparticles. It is worth mentioning that all the spectra exhibit prominent peaks, which are significant in determining the molecular atmosphere of the copper-based materials present on the nanoparticle's surface. For instance, the –OH peak at 3348 cm^{-1} specifies the occurrence of hydroxyl groups, while the stretching vibration of the C = O group at 1635 cm^{-1} signifies the involvement of copper compounds. These findings highlight the valuable information that can be obtained from FTIR spectroscopy when studying copper-based nanomaterials.

Moving on to Figure 2, the SEM images depict the clammy cherry-stabilized CuNPs. These images convey useful information regarding the morphology and structure of the particles. It is intriguing to observe that the clustered CuNPs develop well-defined sphere-shaped microstructures. Furthermore, these microspheres are covered with a thin film consisting of different phytoconstituents found in the gum of the aqueous extract of the cherry. This coating adds an extra layer of complexity to the nanoparticles and may have important implications for their potential applications. The morphology of CuNPs' surface and their elemental configuration were thoroughly explored by employing SEM in combination with energy dispersive X-ray spectroscopy (EDX) analyses. The SEM micrograph images revealed intriguing aggregations of spherical nanoparticles (depicted in Figure 2).

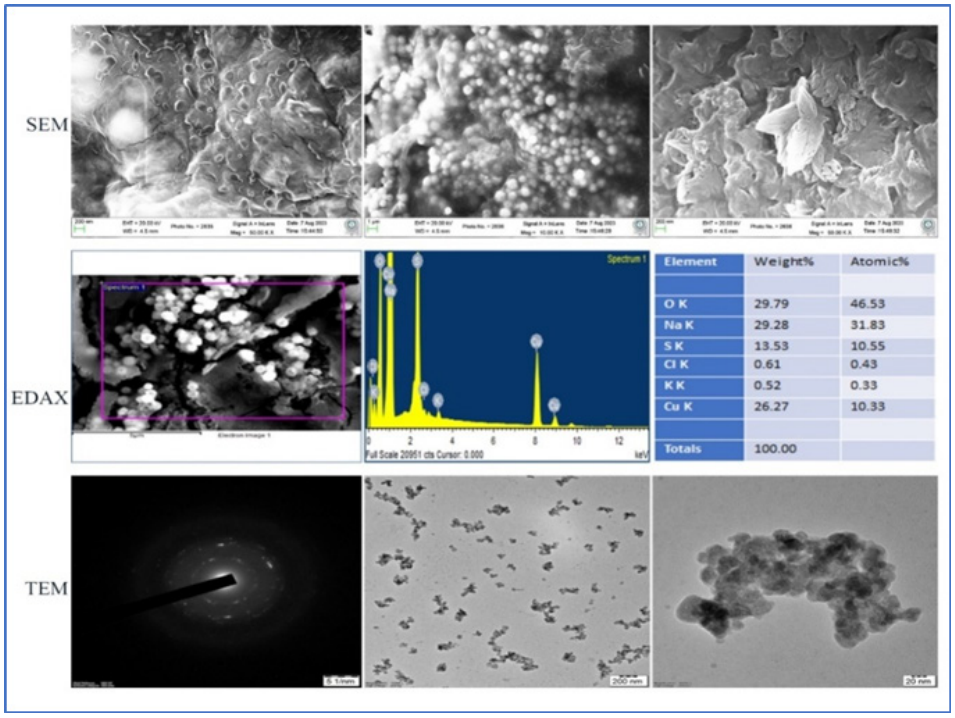

Figure 2: SEM, EDX and TEM of CuNPs synthesised using *H. indicus* leaf extract.

It is important to mention that these aggregates were most likely formed because of the isolation procedures employed for separating CuNPs from the reaction mixtures, which involved a combination of centrifugation and freeze-frying techniques. Furthermore, the EDX analysis provided valuable quantitative and qualitative information regarding the chemical composition of the CuNPs. Upon closer inspection at a magnification of 2 μm, the nanoparticles exhibited an agglomerated spherical form, while at a magnification of 200 nm; they presented a distinctive segregated spherical-shaped structure. To decisively determine the elemental composition of the biosynthesized nanomaterial surfaces, EDAX spectroscopy was employed. The findings garnered from the EDAX spectroscopy showcased the undeniable existence of the copper element, verifying that the biosynthesis process successfully yielded *H. indicus* CuNPs. This finding further bolstered the credibility and efficacy of the biosynthesis technique employed to produce the

nanomaterials. Figure 2 displays a Transmission Electron Microscopy (TEM) micrograph, which effectively portrays the CuNPs that were synthesized. To delve deeper into the characteristics of the synthesized nanoparticles, the researchers conducted a thorough investigation, employing TEM to study their morphology and crystal structure.

Through the TEM image, we were able to identify a few instances of agglomerated CuNPs at specific locations, compelling them to utilize TEM to analyse the size, structure, dispersion, morphology and orientation of both biological and physical materials. Consequently, this analysis indicated the possibility of sedimentation occurring later in the process upon closer examination; it became evident that there existed significant variation in the particle sizes, with the estimated average falling within the range of 10 to 20 nm. Furthermore, it was observed that the enhanced electrostatic attraction between particles played a significant role in their strong aggregation. The smaller size as well as narrower size distribution observed in these nanoparticles was attributed to the rapid reduction facilitated by Microwave (MW) irradiation.[12]

In this study, extensive research to evaluate the antibacterial properties of the CuNPs that were synthesized in vitro. The experimental plant sample activity studies against Gram-positive and Gram-negative bacteria, as well as fungal strains. To test this, we utilized the Mueller-Hinton Agar (MHA) well diffusion method. The bacterial variants with crude plant extract and synthesized CuNPs and then kept for 24 h in the dark at 37°C. The results are represented in Figures 3 and 4.

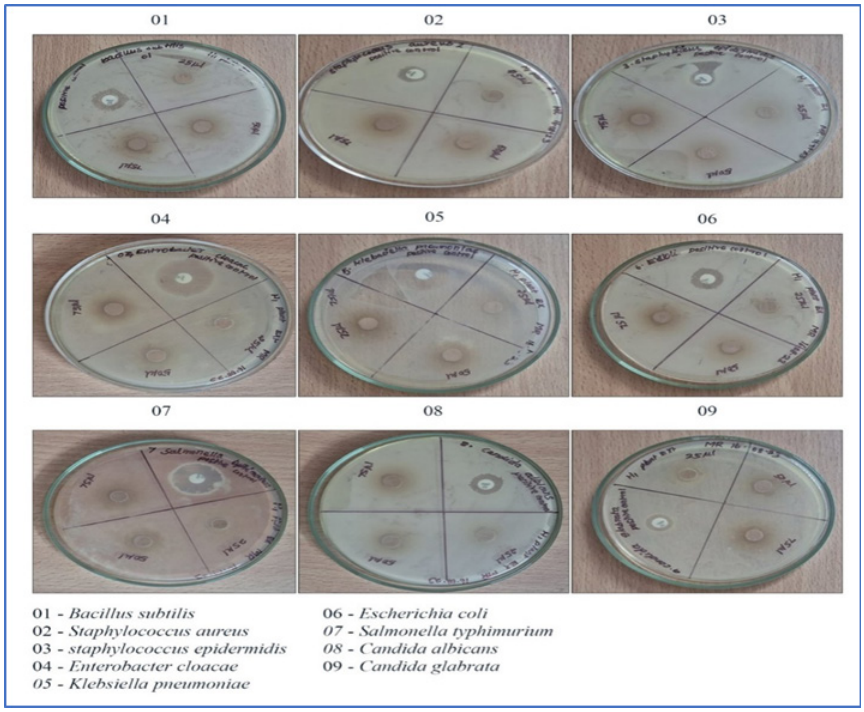

Figure 3: Antimicrobial activity of *H. indicus* plant extract against 9 Organisms.

To present our findings, we organized the results into a table (Table 2) to illustrate the antibacterial properties of the crude plant extract and *H. indicus* CuNPs against several gram-positive and gram-negative organisms, as well as fungi. At a concentration of 75 µL of H1 plant extract, we observed the creation of a zone of inhibition, indicating the effectiveness of the extract against gram-positive microbes including *S. aureus*, *Bacillus subtilis* and *S. epidermidis*. The corresponding inhibition zone measurements for these bacteria were approximately 0.7, 1 and 0.9, respectively, when compared to the control group treated with ampicillin antibiotic.

Similarly, we found that the gram-negative organisms and fungal strains exhibited a high occurrence of zone formation when treated with green-synthesized copper nanoparticles (*H. indicus* CuNPs), as depicted in Figure 4. The effectiveness of the CuNPs was significantly higher than the crude plant extract as antifungal agents was further supported by the results Figure 4.

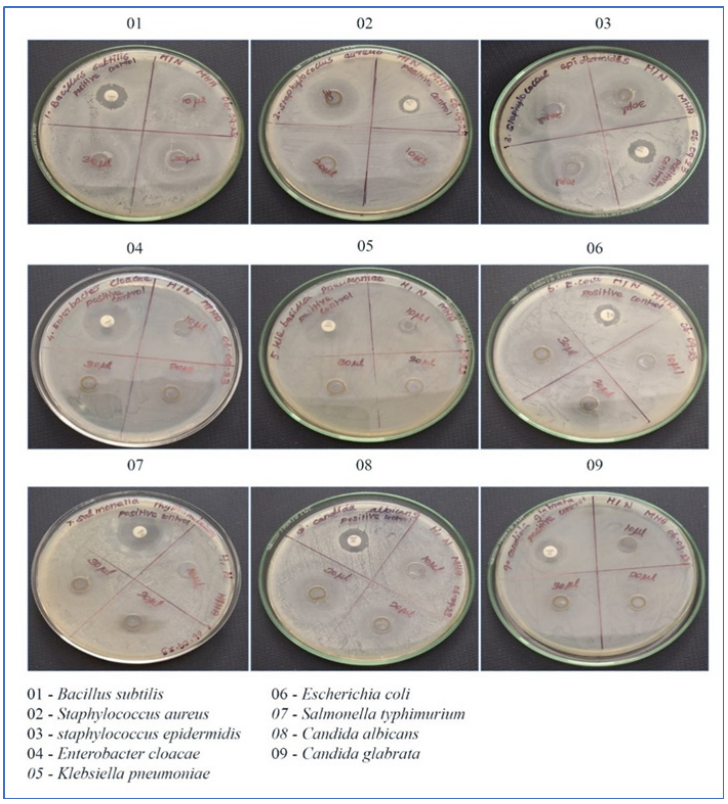

Figure 4: Antimicrobial activity of *H. indicus*-based CuNP against Gram-Positive Organisms

Table 2: Antimicrobial activity of HI plant crude and HICuNP against 9 Organisms.

Sl. No.	Bacterial name	*H. indicus* PLANT EXTRACT (in cm)				H. indicus CuNP (in cm)			
		25 µL	50 µL	75 µL	Ampicillin	Ampicillin	10 µL	20 µL	30 µL
Gram Positive									
1	*B. subtilis*	0.5 ± 0.01	0.6 ± 0.02	0.7 ± 0.02	0.8 ± 0.04	0.4 ± 0.02	1.5 ± 0.04	1.9 ± 0.03	2.1 ± 0.05
2	*S. aureus*	0.6 ± 0.02	0.9 ± 0.04	1 ± 0.05	1 ± 0.02	0.3 ± 0.01	1 ± 0.04	1.2 ± 0.03	1.4 ± 0.04
3	*S.epidermidis*	0.4 ± 0.01	0.6 ± 0.03	0.9 ± 0.03	1 ± 0.03	0.4 ± 0.01	1.8 ± 0.05	2 ± 0.05	2.1 ± 0.05
Gram Positive									
1	*B. subtilis*	0.5 ± 0.01	0.6 ± 0.02	0.7 ± 0.02	0.8 ± 0.04	0.4 ± 0.02	1.5 ± 0.04	1.9 ± 0.03	2.1 ± 0.05
2	*S. aureus*	0.6 ± 0.02	0.9 ± 0.04	1 ± 0.05	1 ± 0.02	0.3 ± 0.01	1 ± 0.04	1.2 ± 0.03	1.4 ± 0.04
3	*S.epidermidis*	0.4 ± 0.01	0.6 ± 0.03	0.9 ± 0.03	1 ± 0.03	0.4 ± 0.01	1.8 ± 0.05	2 ± 0.05	2.1 ± 0.05
Gram Negative									
4	*E. cloacae*	0.6 ± 0.01	0.9 ± 0.02	2 ± 0.04	1 ± 0.04	0.6 ± 0.04	-	-	-
5	*K. pneumoniae*	0.6 ± 0.01	0.6 ± 0.01	1 ± 0.02	1 ± 0.04	0.6 ± 0.04	-	-	-
6	*E.coli*	0.8 ± 0.03	1 ± 0.03	1.1 ± 0.03	0.7 ± 0.03	0.4 ± 0.01	1	1.3 ± 0.03	1.5 ± 0.03
7	*S. Typhimurium*	0.4 ± 0.01	0.7 ± 0.01	0.9 ± 0.01	1.2 ± 0.04	0.8 ± 0.04	-	0.9 ± 0.03	0.5 ± 0.04
Fungi									
8	*C. albicans.*	1 ± 0.04	1.8 ± 0.04	1 ± 0.03	0.6 ± 0.02	0.4 ± 0.01	1.1 ± 0.05	1.2 ± 0.05	1.3 ± 0.03
9	*C. glabrata*	1 ± 0.04	1.4 ± 0.04	0.9 ± 0.03	0.5 ± 0.02	0.4 ± 0.01	-	0.7 ± 0.04	0.8 ± 0.03

Furthermore, we also evaluated the in vitro cytotoxicity of the CuNPs and crude plant extract in A549 cell lines (Figure 5). The evaluation was conducted using various concentrations of the plant extracts (ranges from 100 to 600 µg/mL) and CuNPs (varies from 10 to 50 µg/mL). Each concentration was incubated for 24 hr. To compare the results, we included a control group. The IC_{50} value was then plotted by relating the concentration of crude extract and CuNPs on the X-axis to the percentage of cell viability on the Y-axis.

The samples proved considerable cytotoxicity against the A549 cell proliferation was inhibited by CuNPs having an IC_{50} value of 32 µg/mL. The microscopic analysis demonstrated a reduction in cell density as well as the substrate adhesion ability, along with membrane shrinking, subsequently exposure to a plant extract and *H. indicus* plant-derived CuNPs, with the processes becoming more intensive after 24 hr. The MTT test was utilised to decide the cytotoxicity of CuNP leaf extract on Lung Cancer A549 cells.

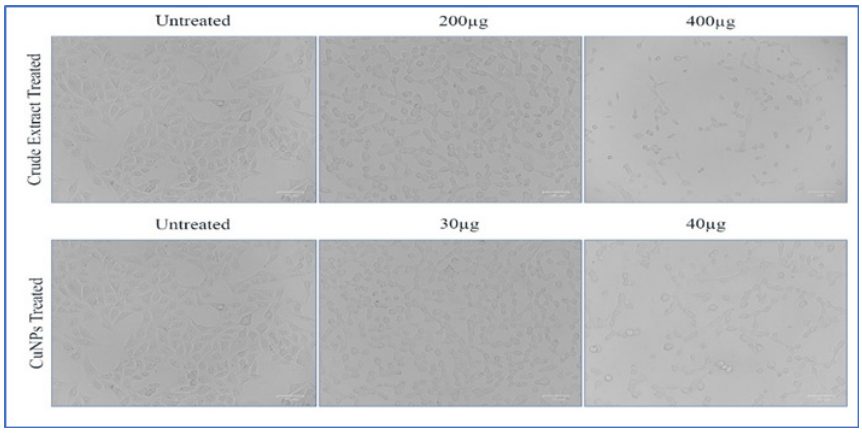

Figure 5: MTT assay-Morphological changes in control, crude plant extract treated *H. indicus* CuNPs treated in Lung Cancer (A549) cells for 24 hr

These morphological alterations are typical for apoptosis and the study used the procedures described below to confirm apoptosis. The dyes used in the experiment were effective in counterstaining the ds-DNA found in the nucleus of both inactive and active cells. Specifically, acridine orange was used by both active as well as dormant cells, while EtBr was exclusively used in nonviable cells. This distinction is because EtBr interacts with DNA and emits red fluorescence, making it a reliable indicator of nonviable cells. The staining process using AO/EtBr supplied valuable insights into the effects of *H. indicus* CuNPs at 32 µg/mL on lung cancer cells. After 24 hr of treatment, it was seen that *H. indicus* CuNPs led to a higher rate of cell death (apoptosis) in lung cancer cells compared to crude plant extract-treated A549 cells (Figure 6).

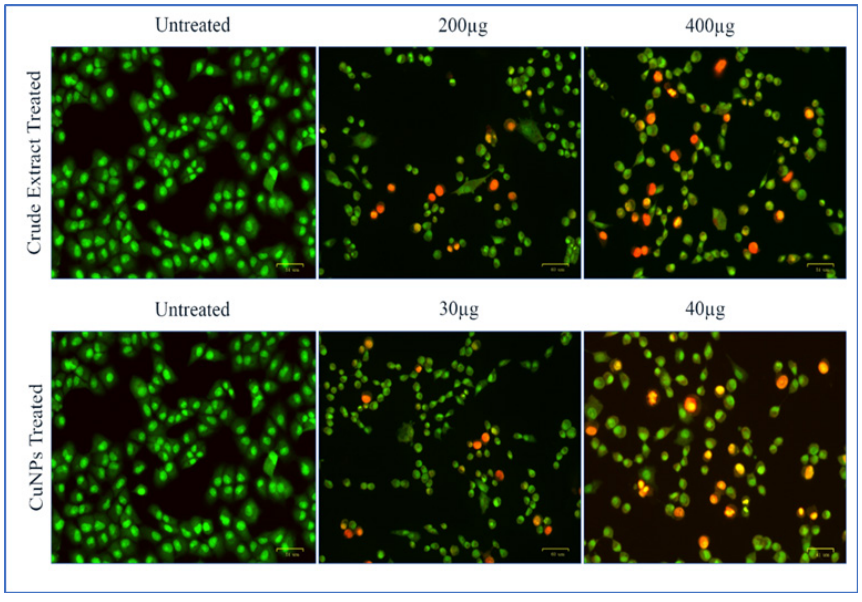

Figure 6

A549 cancer cells, which are commonly used in cancer research, were subjected to treatment with crude plant extract at various concentrations of 200 and 400 µg/mL and *H. indicus*-based CuNPs at multiple concentrations of 20 and 40 µg/mL for 24 hr. Following treatment, the cells were carefully stained using AO/EB, a commonly used staining technique and then underwent analysis using a fluorescence microscope called the Bio-Rad Zoe Fluorescent Cell Imager.

Interestingly, live cells showed green fluorescence and a normal nuclear appearance, showing their healthy state. On the other hand, cells in the initial stages of apoptosis emitted yellow fluorescence and displayed broken nuclei and compacted chromatin. As apoptosis progressed to its late stage, cells displayed orange fluorescence, representing condensation of chromatin or fragmentation, ultimately leading to red/orange-stained cell nuclei. The significant nuclear changes seen in *H. indicus* CuNP-treated cells, such as condensation of chromatin and nuclear disintegration, further confirmed the trigger of cell death through apoptosis. To support these findings, additional staining methods were employed to distinguish between normal and apoptotic cells. Another notable aspect of apoptosis is the stimulation of caspase enzymes, which play a vital role in breaking down essential cellular proteins, specifically targeting the cytoskeleton and nuclear scaffold. Furthermore, caspase enzymes activate DNase, which leads to the destruction of nuclear DNA. To explore the biological markers of apoptosis, a DNA fragmentation test was conducted.

Lung cancer cells were treated with crude plant extract/ IC_{50} and HICuNP/IC50, following which DNA was isolated and examined by employing agarose gel electrophoresis. Through this technique, a characteristic ladder pattern of internucleosomal DNA fragmentation was found in lung cancer cells after treatment with *H. indicus* CuNP/IC50-32 µg/mL (Figure 7). At 32 µg/mL, *H. indicus* CuNPs demonstrated its impact on lung cancer cells by increasing apoptotic proteins and suppressing the PI3K/mTOR pathway. This demonstrated the potential of *H. indicus* CuNPs as a therapeutic agent against lung cancer. Furthermore, the evaluation of cell regulators and apoptotic proteins in lung cancer cells revealed important insights into the cellular mechanisms involved in *H. indicus* CuNP's effects. This allowed for comparison and analysis of the differential impact of each concentration on the lung cancer cells. Interestingly, it was observed that the highest concentrations of leaf extract led to the arrest of cell proliferation, ultimately inducing apoptosis. Building upon these findings, the concentration of 32 µg/mL of *H. indicus* CuNPs was specifically chosen to further investigate its effects on apoptotic proteins and cell regulatory proteins of the PI3K and mTOR pathway in lung cancer cells using RT PCR analysis (Figure 8). The aim was to intensify the activation of the apoptotic pathway to promote cell death in A549 cells, a well-known lung cancer cell line. The results demonstrated that *H. indicus* CuNP treatment was successful in activating the apoptotic pathway in these cells, possibly offering a promising therapeutic approach for lung cancer treatment with more advanced studies.

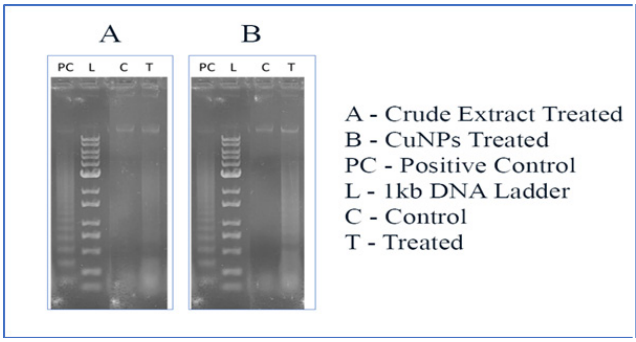

Figure 7: DNA fragmentation assay.

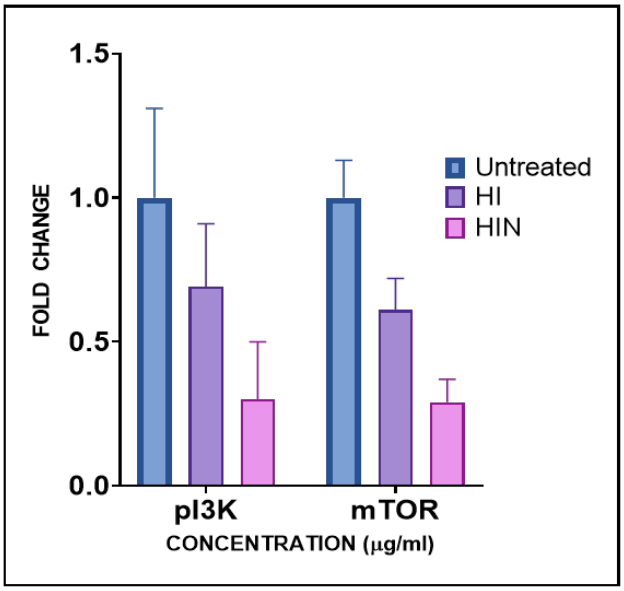

Figure 8: Effect of *H. indicus* CuNPs and crude plant extract in lung cancer cells in down-regulating the anti-apoptotic gene expressions (PI3K and mTOR) by using real-time PCR.

DISCUSSION

Copper nanoparticles have Multiple uses in various industries, comprising cosmetics, biosensing, electronics, textiles, food processing and medical diagnostics. [13-16] These applications stem from their unique properties and potential benefits. It is noteworthy that nanoparticles can be created using several methods, such as physical, chemical, and biological processes. Among these methods, biological approaches are increasingly considered more efficient and eco-friendly. [17] The use of green techniques in the manufacture of CuNPs brings the advantage of improved stability.[4,7,18] Flavonoid biomolecules played a crucial role in the conversion and stabilization of CuNPs. These biomolecules reacted with Cu2+ ions and formed CuNPs. They also stabilized nanoparticles by chelating with metal ions. Its ability to effectively convert metal ions into nanoscale particles with unique shapes and

sizes highlights the potential uses of these particles in different fields such as medicine, energy and electronics. The irregular size and cylindrical shape observed in both studies demonstrate reproducibility and reliability. The process of synthesizing nanoparticles has become an increasingly popular field of research, with scientists constantly seeking new and more sustainable methods to produce these tiny particles.

Overall, this study demonstrates that green synthesis is a promising method for synthesizing Cu NPs, with its ability to effectively produce pure and environmentally friendly nanoparticles. The evaluation of the shapes and sizes of biosynthesized nanoparticles is a crucial aspect of understanding their potential applications. This data is crucial in determining the reactivity and behaviour of these nanoparticles in various environments. The use of copper nanoparticles as a means of combating bacterial infections has acquired significant attention in recent years. This is due in part to the antibacterial properties exhibited by these particles, which are influenced by several key factors. There are three main mechanisms through which these nanoparticles exert their antibacterial action. Initially, they can cause degeneration of the cell wall and cell membrane of bacteria. This is achieved via the interaction between the copper ions on the nanoparticle surface and the phospholipids in the cell wall of bacteria. As a consequence, the structural integrity of the bacteria is compromised, making it more susceptible to other forms of damage. Another way in which these nanoparticles work is by infiltrating the bacterial cells and disrupting their normal functioning.[19,20] Approximately 90% of the populations of B. subtilis, S. aureus and other gram-negative bacteria were reduced. The specific mechanism by which nanoparticles interact with bacteria is not fully comprehended. It is believed that the production of Reactive Oxygen Species (ROS) and the release of Cu ions can disturb the structure of bacterial DNA and cell membranes, leading to the eradication of the bacteria.

CuNPs possess the capability to attach to amine and carboxyl groups. Additionally, it has been observed that when copper nanoparticles are combined with commercial acrylic paint, they exhibit noteworthy antifungal properties. Moreover, copper nanoparticles have a well-documented history of displaying potent antibacterial activity. Remarkably, a recent study proposes that when g-Cu NPs are combined with bioactive compounds derived from other sources, a synergistic effect occurs, resulting in a substantial reduction in the action of pathogenic bacteria.[21] Thus, these findings highlight the potential of using copper nanoparticles in various applications, such as in coatings or paints, to provide enhanced antifungal and antibacterial properties. The current study findings provide promising insights into the potential applications of CuNPs and their bioactive compound counterparts in combating both pathogenic bacteria and cancer cells.

Apoptosis is a highly regulated process that is essential for normal cell development and the elimination of damaged or undesirable cells. The Dysregulation of apoptotic pathways involved in the development and progression of various human malignancies.[12,22,23] Among the intricate signalling pathways involved in cancer, the PI3K/ mTOR pathway stands out as one of the most disrupted. In most malignancies, each core node within the aforementioned pathway exhibits aberrant activity of Cancer Formation and Progression.[24] The activation of PI3Ks, which are key enzymes involved in cellular signalling pathways, leads to the phosphorylation of a specific lipid molecule phosphatidylinositol 4,5-bisphosphate (PIP2). This phosphorylation event converts PIP2 into another lipid molecule known as phosphatidylinositol-3,4,5-triphosphate (PIP3). The formation of PIP3 is significant as it triggers the activation of a protein Akt, also called protein kinase B. When Akt is stimulated, it exerts its influence on various aspects of cancer cell behaviour. One of the main effects of Akt activation is the promotion of cancer cell proliferation, allowing tumours to grow and spread more rapidly. In addition, Akt activation also enhances the survival of cancer cells by preventing apoptosis. Moreover, Akt activation plays a crucial function in regulating the cell cycle, ensuring that cancer cells can continuously divide and proliferate. Furthermore, the PI3K signalling pathway has been associated with a wide range of physiological and pathological activities. In many cases, this pathway becomes dysregulated in cancer settings, leading to its hyperactivation. Numerous human cancers, including ovarian, gastric and breast cancer, have been shown to activate the PI3K/Akt/mTOR pathway and exhibit overexpression of the mTOR, a downstream effector of Akt.[24,25] This activation of Akt influences different aspects of cancer cell behaviour, including proliferation, survival and cell cycle regulation. The study by Zhang *et al.* found that the higher levels of phosphorylated Akt and mTOR of OLP tissues confirmed the presence of stimulated Akt/mTOR autophagy of OLP lesions. The dysregulation of the PI3K/Akt/mTOR signalling pathway has significance in a variety of physiological and pathological processes,

particularly in both the development and progression of malignancies. The investigation on the impact of CuNPs on lung cancer cells revealed a significant decrease in the expression of PI3K, AKT and mTOR proteins, suggesting that CuNPs effectively prevent the growth of lung cancer cells and induce cell death *in vitro*.

Concerning the research findings with *Hemidesmus indicus* (HI), only a few reports were available for nanoparticle synthesis and characterization.[26] Some studies have attempted to understand the phytoactive compounds and antibacterial activities of this plant extract. Recently, it was stated that HI-based gold nanoparticles showed significant antibacterial activity against *P. aeruginosa*.[27] In addition, the same reported that they exhibit nontoxic effects on the human embryonic kidney cells. Thus they proved the *H. indicus*-based gold nanoparticles to be an active antibiofilm agent against P. aeruginosa. In recent reports, HI extracts have been proven to show promising results in treating MRSA infection in combination with amoxicillin/clindamycin.[28] Many other reports also support the antimicrobial action of the *H. indicus* extracts including root and other parts of the plant against a broad range of microbes.[6,29-33]

From the traditional medicine reports, it was observed that H.indicus extracts are known to cure various skin diseases. Incoherent to that, few reports intended to synthesize zinc nanoparticles by using the *H. indicus* extract and characterized them to have a better impact in the field of medicine as well as the pharmaceutical industry.[34] Reports also found that *H. indicus* extract possesses significant secondary metabolites and they were proven to attenuate the growth of cancer cells in the colon.[35]

CONCLUSION

In this comprehensive investigation, an extract derived from the leaves of *H. indicus*, a widely available plant was carefully used to synthesize Copper (Cu) nanoparticles. Advanced methods with FTIR, UV-VIS spectroscopy, SEM and XRD were employed to delve into the characteristics and properties of the resulting Cu nanoparticles. Our results observed that the Cu nanoparticles produced through this innovative methodology displayed remarkable efficacy against a broad spectrum of infections. The multifaceted benefits of these Cu nanoparticles made them a promising solution for combating various infectious agents. Moreover, this ingenious approach boasts a significant advantage in terms of cost-effectiveness.

The researchers observed significant inhibition of bacterial growth with the utilization of these nanoparticles, showcasing their potential as a potent antibacterial agent. Through in-depth experiments and technological analysis, the researchers discovered that these nanoparticles induced apoptosis, or programmed cell death, in lung cancer cells of humans. This discovery sheds light on the cytotoxic aetiology and apoptotic mechanism of *H. indicus* CuNPs in A549 cells, a commonly studied lung cancer cell line. This observation provides insightful information on the potential mechanisms through which *H. indicus* CuNPs exert their anticancer effects. The findings of this research open exciting possibilities for the development of environmentally synthesized *H. indicus* CuNPs as potent anticancer drugs against lung cancer in future. Overall, this comprehensive investigation serves as a valuable contribution to the field of nanotechnology and its diverse applications. The environmentally friendly production of Cu nanoparticles using *H. indicus* (L.) R. Br. not only highlights the potential for sustainable and cost-effective solutions but also showcases the immense promise these nanoparticles hold in various fields, including antimicrobial treatment and cancer therapeutics.

ACKNOWLEDGEMENT

We acknowledge Dr T Balasankar, Clinbiocare Technology, for his support towards Cell culture experiments and analysis.

ABBREVIATIONS

UV: Ultraviolet; **FT-IR**: Fourier Transform Infrared Spectroscopy; **SEM**: Scanning Electron Microscopy; **TEM**: Transmission Electron Microscopy; **MTT**: 3-(4,5-dimethylthiazol-2-yl)-2,5-diphenyltetrazolium bromide; **RT-PCR:** Reverse Transcription Polymerase Chain Reaction; **MHA**: Mueller-Hinton Agar;

SUMMARY

Research into natural chemicals and nanotechnology has led to the synthesis and analysis of copper nanoparticles (CuNPs) using *Hemidesmus indicus* leaf extract, showing significant antimicrobial and anticancer potential. Characterization via UV, FTIR, SEM, SEM-EDAX and TEM revealed CuNPs' efficacy against nine organisms, surpassing crude plant extract. *In vitro* studies on lung cancer cells (A549) demonstrated CuNPs inducing apoptosis, confirmed by nuclear changes and gene expression analysis (RT-PCR) targeting AKT and

mTOR. This study underscores CuNPs derived from *H. indicus* as promising antimicrobial and anticancer agents, highlighting their therapeutic potential.

REFERENCES

1. Gayathri M, Kannabiran K (2009) Antimicrobial activity of *Hemidesmus indicus*, *Ficus bengalensis* and *Pterocarpus marsupium* roxb. Indian Journal of Pharmaceutical Sciences 71(5):578-81. doi:10.4103/0250-474X.58182.
2. Latha M, Sumathi M, Manikandan R, Arumugam A, Prabhu NM (2015) Biocatalytic and antibacterial visualization of green synthesized silver nanoparticles using *Hemidesmus indicus*. Microbial Pathogenesis 82:43-9. doi: 10.1016/j.micpath.2015.03.008.
3. Khanra K, Roy A, Bhattacharyya N (2013) Evaluation of Antibacterial Activity and Cytotoxicity of Green Synthesized Silver Nanoparticles Using. American Journals of Nanoscience and Nanotechnology Research 1:1-6.
4. Iravani S (2011) Green synthesis of metal nanoparticles using plants. Green Chemistry 13(10):2638-50. doi:10.1039/C1GC15386B.
5. Mahalingam G, Kannabiran K (2009) *Hemidesmus indicus* root extract ameliorates diabetes-mediated metabolic changes in rats. International Journal of Green Pharmacy (IJGP) 3(4). doi:10.22377/jpg.v3i4.108.
6. Purohit P, Bais RT, Khan S (2014) Assessment of antibacterial activity and phytochemical screening of *Hemidesmus indicus* root extracts. Pharmaceutical and Biosciences Journal:67-72. doi:10.20510/ukjpb/2/i6/91178.
7. Sivaraj R, Rahman PKSM, Rajiv P, Narendhran S, Venckatesh R (2014a) Biosynthesis and characterization of *Acalypha indica* mediated copper oxide nanoparticles and evaluation of its antimicrobial and anticancer activity. Spectrochimica Acta Part A: Molecular and Biomolecular Spectroscopy 129:255-8. doi:10.1016/j.saa.2014.03.027
8. Rautela A, Rani J, Debnath M (2019) Green synthesis of silver nanoparticles from *Tectona grandis* seeds extract characterization and mechanism of antimicrobial action on different microorganisms. Journal of Analytical Science and Technology 10(1):5. doi:10.1186/s40543-018-0163-z.
9. Abbas S, Nasreen S, Haroon A, Ashraf MA (2020) Synthesis of Silver and Copper Nanoparticles from Plants and Application as Adsorbents for Naphthalene decontamination. Saudi J Biol Sci 27 (4):1016-1023. doi:10.1016/j.sjbs.2020.02.011.
10. Hudzicki J (2009) Kirby-Bauer Disk Diffusion Susceptibility Test Protocol.
11. Ananthi S, Lakshmi CNP, Atmika P, Anbarasu K, Mahalingam S (2018) Global Quantitative Proteomics Reveal Deregulation of Cytoskeletal and Apoptotic Signalling Proteins in Oral Tongue Squamous Cell Carcinoma. Scientific Reports 8(1):1-13 https://www.nature.com/articles/s41598-41018-19937-41593
12. Chen Y-F, Yang J-S, Chang W-S, Tsai S-C, Peng S-F, Zhou Y-R (2013) *Houttuynia cordata* Thunb extract modulates G0/G1 arrest and Fas/CD95-mediated death receptor apoptotic cell death in human lung cancer A549 cells. Journal of Biomedical Science 20(1):18. doi:10.1186/1423-0127-20-18.
13. Ashtaputrey SD, Ashtaputrey PD, Yelane N (2017) Green Synthesis and Characterization of Copper Nanoparticles Derived From *Murraya Koenigii* Leaves Extract. 10(3).
14. Ramyadevi J, Jeyasubramanian K, Marikani A, Rajakumar G, Rahuman AA (2012) Synthesis and antimicrobial activity of copper nanoparticles. Materials Letters 71:114-6. doi:10.1016/j.matlet.2011.12.055
15. Sankar R, Manikandan P, Malarvizhi V, Fathima T, Shivashangari KS, Ravikumar V (2014) Green synthesis of colloidal copper oxide nanoparticles using *Carica papaya* and its application in photocatalytic dye degradation. Spectrochimica Acta Part A: Molecular and Biomolecular Spectroscopy 121:746-750. doi:10.1016/j.saa.2013.12.020
16. Shende S, Ingle AP, Gade A, Rai M (2015) Green synthesis of copper nanoparticles by *Citrus medica* Linn. (*Idilimbu*) juice and its antimicrobial activity. World Journal of Microbiology and Biotechnology 31(6):865-73. doi:10.1007/s11274-015-1840-3
17. Hussain I, Singh NB, Singh A, Singh H, Singh SC (2016) Green synthesis of nanoparticles and its potential application. Biotechnology Letters 38(4):545-60. doi:10.1007/s10529-015-2026-7.
18. Sivaraj R, Rahman PKSM, Rajiv P, Salam HA, Venckatesh R (2014b) Biogenic copper oxide nanoparticles synthesis using *Tabernaemontana divaricate* leaf extract and its antibacterial activity against urinary tract pathogen. Spectrochimica Acta Part A: Molecular and Biomolecular Spectroscopy 133:178-81. doi:10.1016/j.saa.2014.05.048.
19. Jadhav S, Gaikwad S, Nimse M, Rajbhoj A (2011) Copper Oxide Nanoparticles: Synthesis, Characterization and Their Antibacterial Activity. Journal of Cluster Science 22(2):121-9. doi:10.1007/s10876-011-0349-7.
20. Wei Y, Chen S, Kowalczyk B, Huda S, Gray TP, Grzybowski BA (2010) Synthesis of Stable, Low-Dispersity Copper Nanoparticles and Nanorods and their Antifungal and Catalytic Properties. The Journal of Physical Chemistry C 114(37):15612-6. doi:10.1021/jp1055683.
21. Padil VVT, Cernik M (2013) Green synthesis of copper oxide nanoparticles using gum karaya as a biotemplate and their antibacterial application. International Journal of Nanomedicine 8:889-898. doi:10.2147/IJN.S40599
22. Saravanakumar K, Shanmugam S, Varukattu NB, MubarakAli D, Kathiresan K, Wang M-H (2019) Biosynthesis and characterization of copper oxide nanoparticles from indigenous fungi and its effect of photothermolysis on human lung carcinoma. Journal of Photochemistry and Photobiology B: Biology 190:103-9. doi:10.1016/j.jphotobiol.2018.11.017.
23. Mariadoss AVA, Saravanakumar K, Sathiyaseelan A, Venkatachalam K, Wang M-H (2020) Folic acid-functionalized starch encapsulated green synthesized copper oxide nanoparticles for targeted drug delivery in breast cancer therapy. International Journal of Biological Macromolecules 164:2073-2084. doi:10.1016/j.ijbiomac.2020.08.036.
24. Porta C, Paglino C, Mosca A (2014) Targeting PI3K/Akt/mTOR Signaling in Cancer. Frontiers in Oncology 4.
25. Tapia O, Riquelme I, Leal P, Sandoval A, Aedo S, Weber H, Letelier P, Bellolio E, Villaseca M, Garcia P, Roa JC (2014) The PI3K/AKT/mTOR pathway is activated in gastric cancer with potential prognostic and predictive significance. Virchows Archiv 465(1):25-33. doi:10.1007/s00428-014-1588-4.
26. Shekhawat M (2015) Biogenesis of Zinc Oxide Nanoparticles using Aqueous Extracts of *Hemidesmus indicus* (L.) R. Br. International Journal of Research Studies in Microbiology and Biotechnology 1:20-4.
27. Shilpha J, Meyappan V, Sakthivel N (2022) Bioinspired synthesis of gold nanoparticles from *Hemidesmus indicus* L. root extract and their antibiofilm efficacy against *Pseudomonas aeruginosa*. Process Biochemistry 122:224-37. doi:10.1016/j.procbio.022.10.018.
28. Sannat C, Hirpurkar SD, Shakya S, Dutta GK, Roy M, Jolhe DK, *et al*., (2022) Methanolic extract of *Hemidesmus indicus* root augments the antibacterial and antibiofilm activity of amoxicillin and clindamycin against methicillin-resistant Staphylococcus aureus of bovine origin. Letters in Applied Microbiology 75 (6):1579-1589. doi:10.1111/lam.13825.
29. Latha M, Sumathi M, Manikandan R, Arumugam A, Prabhu NM (2015) Biocatalytic and antibacterial visualization of green synthesized silver nanoparticles using *Hemidesmus indicus*. Microbial Pathogenesis 82:43-49. doi:10.1016/j.micpath.2015.03.008.
30. Manohar A, M K, Kumar PV, Ahamed AJ, Ravikumar A, Vinoth A, Priyadharshan M (2023) Investigation of the morphological, optical and antimicrobial properties of Nd-doped ZnO nanoparticles using *Hemidesmus indicus* (L.) R. Br. Root extracts. JOURNAL OF ADVANCED APPLIED SCIENTIFIC RESEARCH 5 (1). doi:10.46947/joaasr512023463.
31. Sujatha sS, J R A. (2010) *In vitro* antibacterial activity on human pathogenic bacteria and larvicidal effect of root from *Hemidesmus indicus* (*Linn.*) on *Culex qinquifasciatus*. *In vitro* antibacterial activity on human pathogenic bacteria and larvicidal effect of root from *Hemidesmus indicus* (Linn) on Culex qinquifasciatus 2:418-24. doi:10.5138/ijpm.2010.0975.0185.02059.

32. Mohan C (2015) Antibacterial activity and phytochemical screening of *Hemidesmus indicus* L. B. Br. International journal of pure and applied bioscience 3:221-5.
33. Saritha K, Rajesh A, Manjulatha K, Setty OH, Yenugu S (2015) Mechanism of antibacterial action of the alcoholic extracts of *Hemidesmus indicus* (L.) R. Br. *ex Schult, Leucas aspera* (Wild.), *Plumbago zeylanica* L. and *Tridax procumbens* (L.) R. Br. ex Schult. Frontiers in Microbiology 6:577. doi:10.3389/fmicb.2015.00577.
34. Turrini E, Calcabrini C, Tacchini M, Efferth T, Sacchetti G, Guerrini A, *et al.* (2018) *In vitro* Study of the Cytotoxic, Cytostatic and Antigenotoxic Profile of *Hemidesmus indicus* (L.) R.Br. (Apocynaceae) Crude Drug Extract on T Lymphoblastic Cells. Toxins 10(2):70. doi:10.3390/toxins10020070.
35. Nutan, Kumar N, Saxena G (2019) Cytotoxic effect of *Hemidesmus indicus* R. Br. on HCT 116 human colon cell lines. The Pharma Innovation Journal 8(1):86-9.

Cite this article: Mary DRK, Sukumar S. Therapeutic Prospective of Synthesized Copper Nanoparticles using Hemidesmus indicus (R.Br.) on Lung Cancer cell Lines (A549) and its Antibacterial Effect against the Clinical Isolates. Asian J Biol Life Sci. 2024;13(1):120-32.